

2. (a) E. Demole, and D. Berthet, *Helv. Chim. Acta*, **54**, 681 (1971); (b) **55**, 1866 (1972).
3. M. Winter, and P. Enggist, *Helv. Chim. Acta*, **54**, 1891 (1971).
4. G. Ohloff, and G. Uhde, *Helv. Chim. Acta*, **53**, 531 (1970).
5. G. Büchi, and H. Wüest, *Helv. Chim. Acta*, **54**, 1767 (1971).
6. K. H. Schulte-Elte, V. Rautenstrauch, and G. Ohloff, *Helv. Chim. Acta*, **54**, 1805 (1971).
7. K. H. Schulte-Elte, B. L. Müller, and G. Ohloff, *Helv. Chim. Acta*, **54**, 1899 (1971).
8. G. Büchi, and J. C. Vederas, *J. Am. Chem. Soc.*, **94**, 9128 (1972).
9. V. Rautenstrauch, *Helv. Chim. Acta*, **56**, 2492 (1973).
10. K. H. Schulte-Elte, B. L. Müller, and G. Ohloff, *Helv. Chim. Acta*, **56**, 310 (1973).
11. (a) K. S. Ayyar, R. C. Cookson, and D. A. Kagi, *J. Chem. Soc. Chem. Commun.*, 161 (1973); (b) *J. Chem. Soc. Perkin 1*, 1727 (1975).
12. W. G. Dauben, A. P. Kozikowski, and W. T. Zimmermann, *Tetrahedron Lett.*, 515 (1975).
13. S. Torii, K. Uneyama, and H. Ichimura, *J. Org. Chem.*, **44**, 2922 (1979).
14. S. Torii, T. Inokuchi, and H. Ogawa, *J. Org. Chem.*, **44**, 3412 (1979).
15. S. Isoe, S. Katsumura, and T. Sakan, *Helv. Chim. Acta*, **56**, 1514 (1973).
16. C. Fehr, and J. Galindo, *Helv. Chim. Acta*, **69**, 228 (1986).
17. J. D. Surmatis, A. Walser, J. Gibas and R. Thommen, *J. Org. Chem.*, **35**, 1053 (1970).
18. H. Rubinstein, *J. Org. Chem.*, **27**, 3886 (1962).
19. H. J. Liu, H.K. Jung, G. L. Mhehe, and M. L. D. Weiberg, *Can. J. Chem.*, **56**, 1368 (1978).
20. J. J. Eisch, and A. M. Jacobs, *J. Org. Chem.*, **28**, 2145 (1963).
21. W. G. Dauben, M. E. Lorber, N. D. Vietmeyer, R. H. Shapiro, J. H. Duncan, and K. Tomer, *J. Am. Chem. Soc.*, **90**, 4762 (1968).
22. K. J. Kolonko and R. H. Shapiro, *J. Org. Chem.*, **43**, 1404 (1978).
23. A. L. Gemal, and J. L. Luche, *J. Am. Chem. Soc.*, **103**, 5454 (1981).
24. (a) W. G. Dauben and G. A. Boswell, *J. Am. Chem. Soc.*, **79**, 5578 (1957); (b) *J. Am. Chem. Soc.*, **83**, 5003 (1961).
25. (a) R. V. Hoffman, R. D. Bishop, P. M. Fitch, and R. Hardenstein, *J. Org. Chem.*, **45**, 917 (1980); (b) G. W. Francis, and J. F. Berg, *Acta Chem. Scand. B*, **31**, 721 (1977).
26. G. L. O'Conner, H. R. Nace, *J. Am. Chem. Soc.*, **77**, 1578 (1955).
27. The ratio of **13** and **10** in the mixture was estimated approximately 98:2 by glc.

Catalytic Activity of $\text{Nd}_{1-x}\text{Sr}_x\text{CoO}_{3-y}$ on the Oxidation of Carbon Monoxide

Keu Hong Kim*, Seong Han Kim, Dong Hoon Lee, Yoo Young Kim, and Jae Shi Choi

Department of Chemistry, Yonsei University, Seoul 120-749. Received July 30, 1990

The catalytic activity of $\text{Nd}_{1-x}\text{Sr}_x\text{CoO}_{3-y}$, $0 \leq x \leq 0.75$ and $0.001 \leq y \leq 0.103$, on the oxidation of carbon monoxide has been investigated from the structure analyses of the catalysts by X-ray diffraction and infrared spectroscopy and the measurements of the oxidation and adsorption rates of carbon monoxide. The catalytic activity is found to be correlated with Sr substitution (x) and nonstoichiometry (y). The oxidation power of carbon monoxide increases continuously with increasing Sr substitution without oxygen, but increases with Sr substitution up to $x=0.25$ and then is almost constant at larger x values up to $x=0.75$ with oxygen. This change of catalytic activity is explained by the oxidation-reduction properties of the catalyst due to the variation of nonstoichiometry.

Introduction

In metallic oxides the electronic factors are not dependent upon the type, but are closely linked to the properties of the metallic oxides. The catalytic activities of metallic oxides are therefore related to their nonstoichiometric composition and electronic properties. The catalytic oxidation of carbon monoxide on metallic oxide as a catalyst is useful to understand the physicochemical properties of metal oxide. A correlation between the catalytic activity and the d-electron configuration was found to exist in metallic oxide catalyst. Derouane¹ reported that the catalytic activity of metallic oxide on the oxidation of carbon monoxide increases with increase in the empty d-orbital of metal ion.

Perovskite-type mixed oxide NdCoO_{3-y} is suitable catalyst for the basic investigation of the relationships between the physicochemical property of metal oxide and the catalytic activity, since its bulk structure has been well characterized and the number of oxygen vacancies are easily controlled by the incorporation of the foreign element without changing the fundamental structure². The catalytic activities of perovskite oxides have been interpreted by Voorhoeve *et al.*^{3,4} as the backbonding between d-orbital of metal ion and π^* -orbital of carbon monoxide on the oxidation of carbon monoxide.

In this work, we have investigated the catalytic activity of $\text{Nd}_{1-x}\text{Sr}_x\text{CoO}_{3-y}$ catalyst on the oxidation of carbon monoxide from the measurements of the oxidation rates of carbon monoxide and adsorptions of CO and O₂ under various CO

and O_2 pressures. The relation between catalytic activity and Sr substitution has been studied based on changes in the oxidation state of Co and in the concentration of oxygen vacancy.

Experimental

Catalysts. $NdCoO_{3-y}$, $Nd_{0.75}Sr_{0.25}CoO_{3-y}$, $Nd_{0.50}Sr_{0.50}CoO_{3-y}$, and $Nd_{0.25}Sr_{0.75}CoO_{3-y}$ were prepared from chemically pure Nd_2O_3 , $SrCO_3$ and CoO . Appropriate weights of the oxide powders were weighed precisely, mixed in ethanol solution and stirred for 72 h to obtain a homogeneous dispersion. The mixture was then filtered and dried at $150^\circ C$. This mixed powder was put on a covered platinum crucible, placed in a preheated furnace, and sintered in air pressure at $1050^\circ C$ for 20 h and then slowly cooled to room temperature. The sintered powder was ball-milled for 2 h, calcined at $850^\circ C$, and then cooled rapidly to room temperature.

Carbon Monoxide and Oxygen. Carbon monoxide was prepared from the reaction of $CaCO_3$ and Zn powder in mole ratio of 1:2. The chemical reaction was performed by heating them at about $650^\circ C$ in quartz tube. Carbon monoxide was purified with glass wool, KOH and $CaCl_2$. Oxygen was made from heating $KClO_3$ with MnO_2 at about $270^\circ C$. It was purified with glass wool and P_2O_5 . The analyses of reactant gases, CO and O_2 were carried out with gas chromatography using porapak Q column. The purities of CO and O_2 were higher than 99.3 and 99.2%, respectively.

Structure Analysis. X-ray diffraction analysis was carried out on a diffractometer (Philips, PW 1710, $CuK\alpha$) equipped with a curved graphite monochromator in a selected beam path. Based on powder X-ray diffraction data, the accurate lattice parameter (a) for each sample was determined in the same manner as described elsewhere⁵⁻¹⁰. In the diffraction angle analysis, the absorption, sample eccentricity, radius and beam-divergence errors were considered in order to obtain accurate lattice parameters. In this work, a determination of an exact a -value for each sample was made by the Nelson-Riley method¹¹. The lattice parameter (7.548 Å) of pure $NdCoO_{3-y}$ obtained from the Nelson-Riley method nearly agrees with the ASTM listing ($a=7.546$ Å). Determinations of the a -values for various Sr-substituted samples were also carried out by the same method. The a -values obtained for the $Nd_{1-x}Sr_xCoO_{3-y}$ systems are plotted against atomic mol fraction (x) of Sr. The infrared spectra of crystals extracted from KBr pellets were recorded at room temperature on a Shimadzu IR-435 spectrometer¹². In order to obtain informations for microcrystal structure and substitution site of Sr-substituted $NdCoO_{3-y}$ catalysts, the infrared spectra of pure CoO and Co_3O_4 were also recorded at room temperature.

Surface Area, x and y Values. The surface area of each sample (100-160 mesh) was measured by a Blain test. The measured surface area increases with increasing x value, showing 2.01 ($x=0$), 3.87 ($x=0.25$), 4.93 ($x=0.50$) and 5.05 m^2/g ($x=0.75$), respectively. The x value in $Nd_{1-x}Sr_xCoO_{3-y}$ was confirmed by atomic absorption spectroscopy. The non-stoichiometry (y) was calculated by determining the amount of Co^{4+} and the total amount of Co. The total amount of Co was determined following the procedure reported by Gušee *et al.*¹³. The amounts of Co^{4+} and Co^{3+} were also deter-

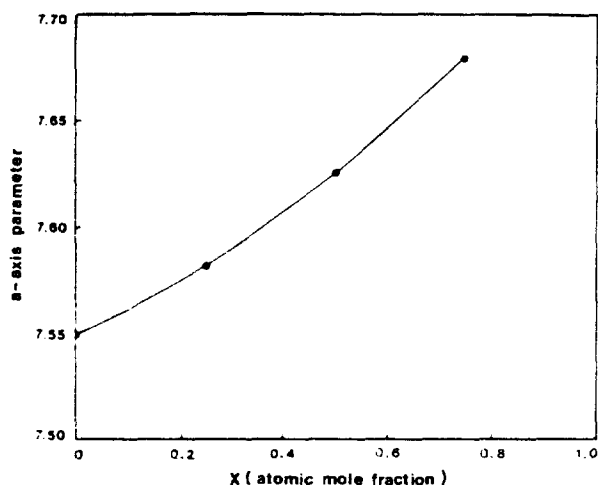


Figure 1. Dependence of the lattice parameter(a) on the amount of Sr in $Nd_{1-x}Sr_xCoO_{3-y}$ catalysts.

mined according to the reported procedure¹⁴. The effective values of x are 0.247, 0.493, and 0.739 in accordance with the nominal values of 0.250, 0.500 and 0.750, respectively. Based on the AAS data, the effective values of x are almost the same as the nominal values. The values of y are 0.001 ($x=0$), 0.008 ($x=0.247$), 0.059 ($x=0.493$), and 0.103 ($x=0.739$), respectively.

Measurements of Adsorption and Oxidation Rates.

The adsorptions of CO and oxygen and the rates of CO oxidation were measured in a completely closed reactor with a total volume of 146 ml. The each powder catalyst was placed in the reaction chamber and sintered at $400^\circ C$ under 10^{-3} Torr for 30 min, and then cooled to room temperature before the reactants were introduced. The reaction chamber was then placed in an electric furnace maintained at a constant temperature controlled within $\pm 0.5^\circ C$. In each run, 0.4-0.5g of catalyst was distributed uniformly in the reaction chamber bed. The initial pressure of the reactant mixture ($2CO+O_2$) was 225 Torr at each reaction temperature. Conversion of CO was monitored by the pressure change at regular time intervals and read by scaled microscope. The rates of CO oxidation reaction were measured by the pressure decrease of reactants, where product CO_2 was condensed by a trap kept at liquid nitrogen temperature. Then the amount of CO_2 formed, which was collected at a trap, was measured. The amount of CO and O_2 consumption was calculated from the pressure decrease and the amount of CO_2 formed. The total pressure decrease and the amount of CO_2 formed were measured after 30 min for each run.

Results and Discussion

The lattice parameter, as can be seen in Figure 1, increases with increase in x . This result is easily explained by the fact that the ionic radius of Nd^{3+} (104 pm) is smaller than that of Sr^{2+} (112 pm) so that the lattice parameter increases somewhat upon addition of Sr. Based on this data, it is possible to determine whether the cubic $NdCoO_{3-y}$ forms solid solution by addition of dopant Sr. However, the plot of lattice parameter *vs.* x does not give straight line, as shown in Figure 1. This implies that the structure of

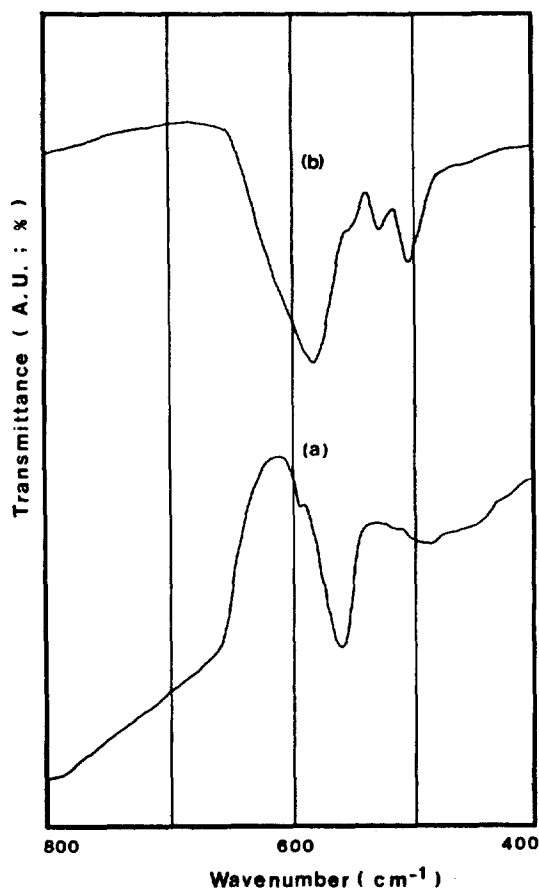


Figure 2. Infrared spectra of CoO(a) and Co_3O_4 (b).

present sample is somewhat distorted cubic.

Figure 2 shows the infrared spectra of CoO(a) and Co_3O_4 (b). As can be seen in Figure 2(a), a single absorption band appears at 560 cm^{-1} . This absorption band is assigned to Co-O vibration due to CoO_6 , since CoO has NaCl structure. As shown in Figure 2(b), the four absorption bands are observed. This is because the Co_3O_4 has spinel structure in which Co^{3+} and Co^{2+} locate at octahedral and tetrahedral sites, respectively. The two infrared bands at 510 and 580 cm^{-1} are considered to be due to the Co-O vibrations of Co^{2+}O_4 and Co^{3+}O_6 in the normal spinel structure, respectively. The remaining two infrared bands at 530 and 560 cm^{-1} are possibly originated from the inverse spinel structure in which some of the Co^{3+} ions move to the tetrahedral sites. From the four observed infrared bands, it is found that the present Co_3O_4 is slightly deviated from the normal spinel structure.

Figure 3 shows the infrared spectra of $\text{Nd}_{1-x}\text{Sr}_x\text{CoO}_{3-y}$ for $x=0$ (a), $x=0.25$ (b), $x=0.50$ (c), and $x=0.75$ (d), respectively. The structure of NdCoO_{3-y} is pseudo-cubic, however, the octahedral symmetry of Co is continuously maintained. As can be seen in Figure 2, the vibrational band due to octahedral Co is observed at average frequency of 570 cm^{-1} . However, the infrared band due to same octahedral Co in NdCoO_{3-y} appears at 470 cm^{-1} , as shown in Figure 3. The infrared band at 570 cm^{-1} due to Co-O vibrations in CoO and Co_3O_4 is somewhat different from the band at 470 cm^{-1} due to Co-O vibrations in NdCoO_{3-y} . This implies that the bond nature of Co-O in CoO and Co_3O_4 is different from

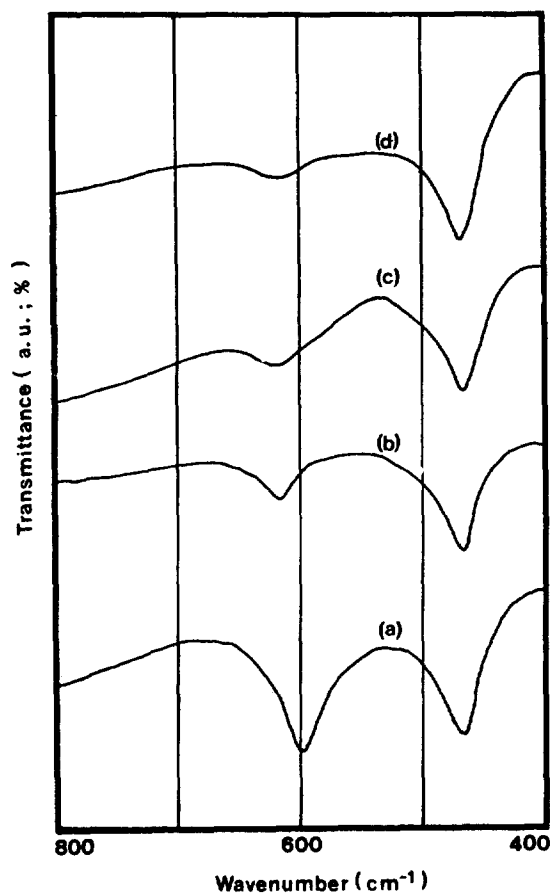


Figure 3. Infrared spectra of $\text{Nd}_{1-x}\text{Sr}_x\text{CoO}_{3-y}$: (a) $x=0$; (b) $x=0.25$; (c) $x=0.50$; and (d) $x=0.75$ atomic mol fraction.

that in NdCoO_{3-y} . On the other hand, in Figure 3, the intensities and frequencies of the 470 cm^{-1} bands are almost unchanged as the amount of Sr incorporated in NdCoO_{3-y} increases, but those of 600 cm^{-1} bands are varied. This indicates that the band at 600 cm^{-1} is originated from Nd-O vibration in NdCoO_{3-y} and implies that the Sr incorporated in NdCoO_{3-y} enters into the Nd site and then increases the nonstoichiometry.

Figure 4 shows the amounts of CO adsorbed as a function of time at 250°C in the reduction of the catalysts by CO. From the slopes of the curves in Figure 4, the initial rates of the CO-reduction increase with increasing amount of Sr incorporated in NdCoO_{3-y} . As can be seen in Figure 4, the adsorption of CO on catalyst is saturated after the initial CO-reduction. This implies that the reduction of the present catalyst by CO is enhanced by the incorporation of Sr. In other words, the nonstoichiometry(y) due to Sr-incorporation increases the adsorption of CO on catalyst, indicating the possible enhancement of catalytic activity.

On the other hand, as shown in Figure 5, the oxygen consumption as a function of time at 250°C in the oxidation of the catalyst by O_2 , the initial rates increase with increasing amount of Sr incorporated in NdCoO_{3-y} and then is saturated after initial oxidation by O_2 . This means that the oxidation power of the catalyst by O_2 is originated from the nonstoichiometry(y) of the catalyst due to the Sr-incorporation. Based on these data in Figure 5, it is possible to say that

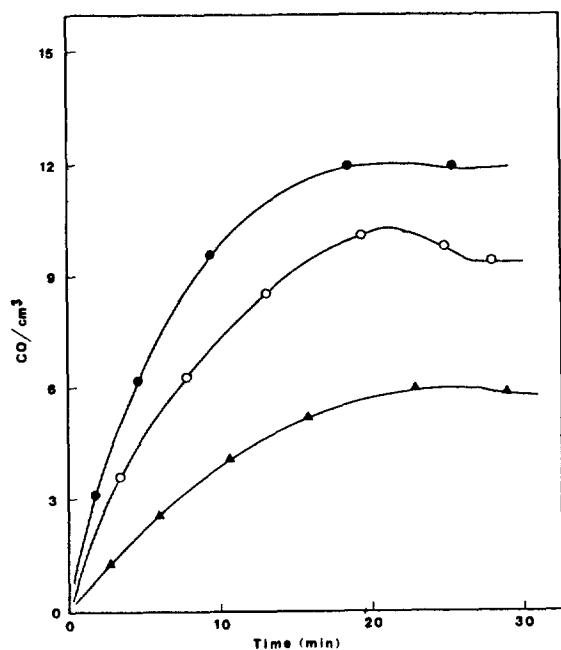


Figure 4. Reduction of $\text{Nd}_{1-x}\text{Sr}_x\text{CoO}_{3-y}$ catalyst by CO: Amounts of CO adsorbed as a function of time at 250°C; Catalyst weight: 0.5g ($x=0.25$, \blacktriangle), 0.4g ($x=0.50$, \circ and $x=0.75$, \bullet).

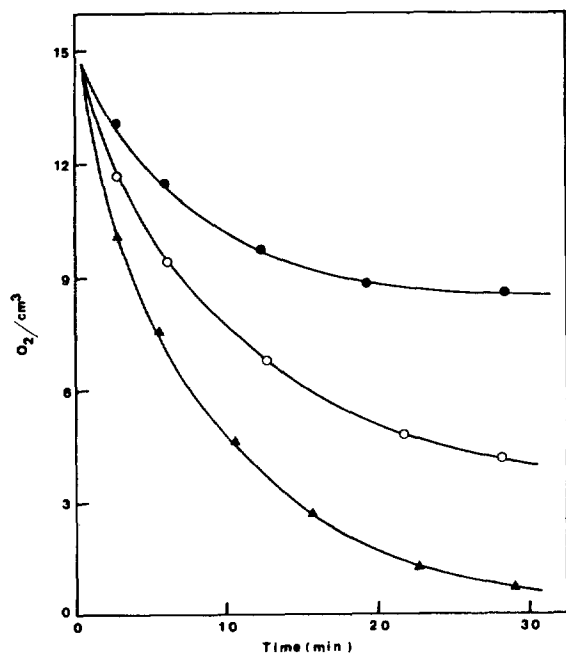


Figure 5. Oxidation of $\text{Nd}_{1-x}\text{Sr}_x\text{CoO}_{3-y}$ catalyst by O_2 : O_2 consumption vs. time at 250°C; catalyst weight: 0.5g ($x=0.25$, \bullet), 0.4g ($x=0.50$, \circ and $x=0.75$, \blacktriangle).

the enhancement of catalytic activity depends upon the degree of nonstoichiometry.

Figure 6 shows the amounts of CO_2 produced from the oxidation of CO without O_2 as a function of Sr incorporated at three different temperatures. The amounts of CO_2 increase with increasing temperature and amounts of Sr incorporated. In other words, the isothermal activity of catalyst depends upon the degree of nonstoichiometry, showing that the

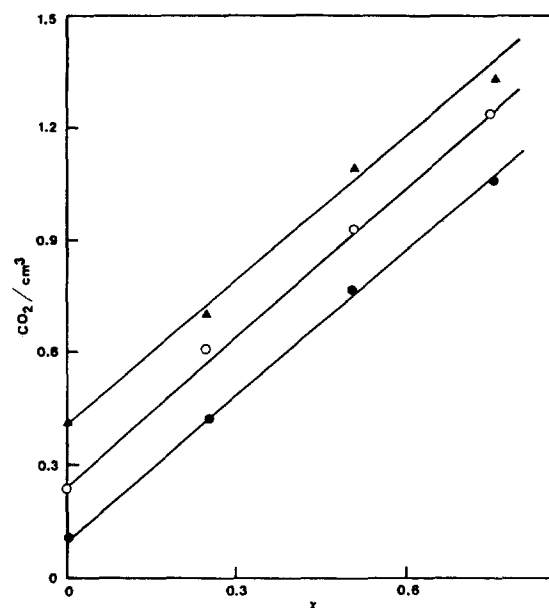


Figure 6. Amounts of CO_2 produced plotted as a function of Sr at 200°C (\bullet), 250°C (\circ), and 300°C (\blacktriangle), Catalyst weight: 0.5g ($x=0.25$), 0.4g ($x=0.50$ and $x=0.75$).

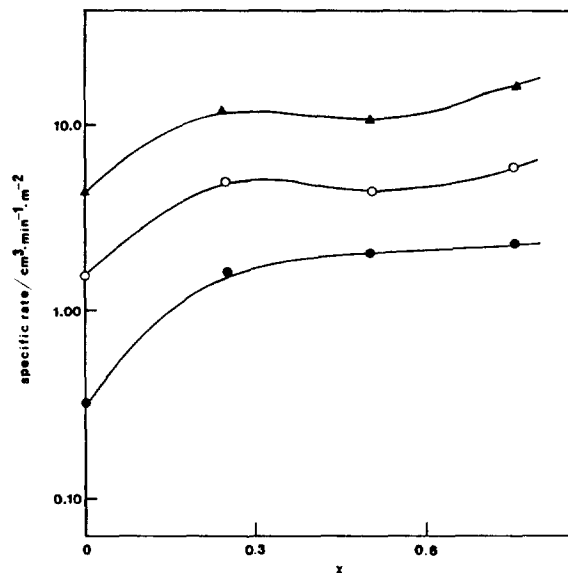


Figure 7. The specific rate vs. x at 200°C (\bullet), 250°C (\circ), and 300°C (\blacktriangle). Catalyst weight: 0.5g ($x=0.25$), 0.4g ($x=0.50$ and 0.75).

amounts of product increase with increasing y values due to increased atomic mol fraction of Sr.

Figure 7 shows the reaction rates of the catalytic oxidation of CO as a function of x . The rate increases with x up to $x=0.25$ and becomes nearly independent on x or decreases slightly with further increase in x up to $x=0.50$. This is very contrast to the fact that when the CO is thermally activated in the absence of O_2 , CO_2 production increases continuously with increasing x in the three cases at all temperatures measured. This extent of CO_2 formation reflects the oxidation power of catalyst.

In conclusion, the catalytic activity of the present $\text{Nd}_{1-x}\text{Sr}_x$

CoO_{3-y} on the oxidation of CO is determined by the degree of nonstoichiometry due to the incorporation of foreign atom such as Sr.

Acknowledgement. The financial support of the Korea Science and Engineering Foundation is greatly acknowledged. The authors are grateful to Drs. H. J. Won, S. K. Cho, and T. J. Kim for helpful assistances of the experiments.

References

1. E. G. Derouane, *Ind. Chim. Belg.*, **36**, 359 (1971).
2. R. J. H. Voorhoeve, "Advanced Materials in Catalysis", p. 129. Academic Press, New York, 1977.
3. R. J. H. Voorhoeve, D. W. Johnson, J. P. Remeika, Jr., and P. K. Gallagher, *Science*, **195**, 827 (1977).
4. R. J. H. Voorhoeve, D. P. Remeika, and L. E. Trimble, *Ann N. Y. Acad. Sci.*, **272**, 3 (1976).
5. K. M. Choi, K. H. Kim, and J. S. Choi, *J. Phys. Chem. Solids*, **49**, 1027 (1988).
6. P. V. Huong, E. Oh-Kim, K. H. Kim, D. Kim, and J. S. Choi, *J. Less-Common Met.*, **151**, 133 (1989).
7. K. H. Kim, D. Y. Yim, K. M. Choi, J. S. Choi, and R. G. Sauer, *J. Phys. Chem. Solids*, **50**, 1027 (1989).
8. D. Kim, K. M. Choi, K. H. Kim, and J. S. Choi, *ibid.*, **50**, 821 (1989).
9. K. H. Kim, S. H. Park, J. S. Choi, and K. W. Hyung, *ibid.*, **49**, 1019 (1988).
10. H. J. Won, S. H. Park, K. H. Kim, and J. S. Choi, *ibid.*, **48**, 383 (1987).
11. J. B. Nelson and D. P. Riley, *Proc. Phys. Soc. (Lond.)*, **57**, 160 (1945).
12. Y. Y. Kim, K. H. Kim, and J. S. Choi, *J. Phys. Chem. Solids*, **50**, 903 (1989).
13. B. E. Gushee, L. Katz, and R. Ward, *J. Am. Chem. Soc.*, **79**, 5601 (1957).
14. H. A. Laitinen and L. W. Burdett, *Anal. Chem.*, **23**, 1268 (1951).

The Approximate Electronic Solutions in A Closed Form, for f.c.c., b.c.c. and h.c.p. Clusters

Gean-Ha Ryu and Hojing Kim*

Department of Chemistry, Seoul National University, Seoul 151-742. Received August 1, 1990

A cluster made of N_A , N_B and N_C atoms in the x , y and z directions respectively, is treated with Hückel method. We obtain the approximate expressions for the eigenvalues and eigenvectors of f.c.c., b.c.c. and h.c.p. clusters in closed forms. The maximum and minimum values of the band so obtained converge to those derived from the Bloch sum in the limit of infinite extension. For a small cluster (of $9 \times 9 \times 5$ atoms, for instance), LDOS from the analytical (approximate) solution manifests better agreement at the surface, than inside the bulk.

Introduction

There are two main streams in assessing the interaction between an adsorbate and a solid substrate. The methods of solid state physics¹⁻³ treat the substrate as a semi-infinite solid, which has infinite extent in the $\pm x$, $\pm y$, and $-z$ direction and has surface at $z=0$, or as *slab*, which is a solid of finite thickness Δz but has infinite extent in the $\pm x$ and $\pm y$ directions. On the other hand, the methods of molecular quantum theory⁴⁻⁶ approximate the metal substrate as a cluster of finite number of atoms.

One question which immediately comes to mind with regard to cluster representing a metal substrate is: how many atoms are needed in the cluster to *describe the metal*? The answer to this question will obviously depend upon which properties of metal one wishes to describe. Empirically,⁷⁻⁹ it is known that localized effects, such as metal-adsorbate bonding, can be treated successfully with a moderate size of cluster which is within a computational reach through most molecular orbital methods. However a cluster of 50 atoms or less, which is already quite a computational feat,

would be sorely inadequate for the discussion of a number of solid state aspects of the substrate, such as bulk cohesive energies and work functions. In practice, therefore, one should investigate and justify the convergence of results as a function of cluster size. It would be very convenient, if one has an analytical measure, to treat a cluster of an arbitrary size, in a consistent way. In a limit of infinite size, the method should reproduce the results derived from bulk solid.

Using simple Hückel theory, Messmer¹⁰ had shown that for a simple cubic (s.c.) array of atoms, the eigenvalues and eigenvectors can be obtained in a closed form for any size of cluster up to the infinite solid.

Here an extension of this to other lattices is intended. That is, the solution of closed form is pursued, within a framework of Hückel theory. The major obstacle is a large coordination number (12 for face centered cubic, while 6 for simple cubic) which leads to an unfavorable form of the secular matrix. A cluster of average configuration is thus conjectured, and there results energy matrix of manageable form. Analytic (Hückel type) solutions for face centered cubic